FEBS Letters 579 (2005) 948–954 FEBS 29106

Minireview

From peptide-bond formation to cotranslational folding: dynamic, regulatory and evolutionary aspects

David Baram, Ada Yonath*

Department of Structural Biology, The Weizmann Institute, 76100 Rehovot, Israel

Received 25 October 2004; revised 25 October 2004; accepted 2 November 2004

Available online 2 December 2004

Edited by Gunnar von Heijne and Anders Liljas

Abstract **Ribosomes are ribozymes exerting substrate positioning and promoting substrate-mediated catalysis. Peptide-bonds are formed within a symmetrical region, thus suggesting that ribosomes evolved by gene-fusion. Remote interactions dominate substrate positioning at stereochemistry suitable for peptide-bond formation and elaborate architectural-design guides the processivity of the reaction by rotatory motion. Nascent proteins are directed into the exit tunnel at extended conformation, complying with the tunnel's narrow entrance. Tunnel dynamics facilitate its interactive participation in elongation, discrimination, cellular signaling and nascent-protein trafficking into the chaperon-aided folding site. Conformational alterations, induced by ribosomal-recycling factor, facilitate subunit dissociation. Remarkably, although antibiotics discrimination is determined by the identity of a single nucleotide, involved also in resistance, additional nucleotides dictate antibiotics effectiveness.**

Keywords: Ribosomal catalysis; Antibiotics selectivity; Ribosome evolution; Trigger factor; Ribosome-recycling factor

1. Symmetry within the asymmetric ribosome

The ribosome, a 2.5 MDa riboprotein assembly is a ribozyme composed of two unequal subunits that associate upon the initiation of the biosynthetic cycle. m-RNA is being decoded at the small subunit, and the peptide bond is being formed by the large one, in the lower end of a cavity built mainly of ribosomal RNA. A single protein, L16 (*Escherichia coli* nomenclature is used throughout), placed at its upper rim (Fig. 1a). Despite the ribosome asymmetric nature, a sizable symmetry-related region relating RNA backbone fold and nucleotides orientations, rather than nucleotides identities, was revealed around the peptidyl transferase catalytic site (PTC) in all known structures (Fig. 1b) [1]. The symmetry-related region contains 180 nucleotides and extends far beyond the PTC. It connects all functional centers involved in amino-acid polymerization, including peptide-bond formation and decoding sites, as well as the RNA entry and leaving regions (Fig. 1b). Ribosomal proteins contacting its exterior [2] include protein L2, residues 228, 229. These contacts are likely to stabilize the region's confirmation, consistent with the essentiality of histidine sidechain at L2-229 for nascent-chain elongation [4], although single peptide bonds can form by protein-free 23S RNA. Similarly, a Zn containing protein (L36) that exists in several species including *Deinococcus radiodurans* binds to the region's non-symmetrical extensions that interact with the elongation factors [2], seems to contribute to the region's stability.

The bond connecting the universally conserved single-strand tRNA-CCA-end with the tRNA-acceptor-stem almost coincides with the symmetry-axis [1,6], indicating that translocation involves two synchronized motions: a rotation of the tRNA 3′ end and an overall mRNA/tRNA sideways shift. Guided by PTC components, which create its template (Fig. 1c), the rotatory motion results in stereochemistry suitable for peptide-bond formation and for nascent-chain elongation [1,5–7]. Furthermore, it places the A-site nucleophilic amine and the P-site carbonyl-carbon at a distance reachable by the P-site tRNA A76 O2′, consistent with its participation in the peptide-bond formation catalysis [8,9] as well as with recent biochemical and kinetic findings [10–12]. Hence, the ribosomal architecture provides all of the positional elements required for aminoacid polymerization.

The PTC symmetrical properties suggest that the ribosomal active site evolved by gene fusion of two separate domains of similar structures, each hosting part of the catalytic activity. The preservation of three-dimensional structure of the symmetrical region despite the lack of sequence identity demonstrates the superiority of the architectural RNA elements that determine the functional efficiency. Protein L16, the only ribosomal protein contributing to tRNA positioning [1,2] shares similar properties, namely its three-dimensional structure is conserved in eubacteria and archaea (Fig. 1a) [3], regardless of the significant variability in the aminoacid sequences. Thus, verifying the dominance of the rigorous requirements for accurate substrate positioning throughout evolution.

2. Positioning hierarchy

The geometrical requirements for a successful rotatory motion are proper A-site binding and initial P-site-tRNA at the rotated conformation. For this aim the PTC offers two

*Corresponding author. Fax: +972 8 9343028.
E-mail address: ada.yonath@weizmann.ac.il (A. Yonath).

0014-5793/$30.00
doi:10.1016/j.febslet.2004.11.063

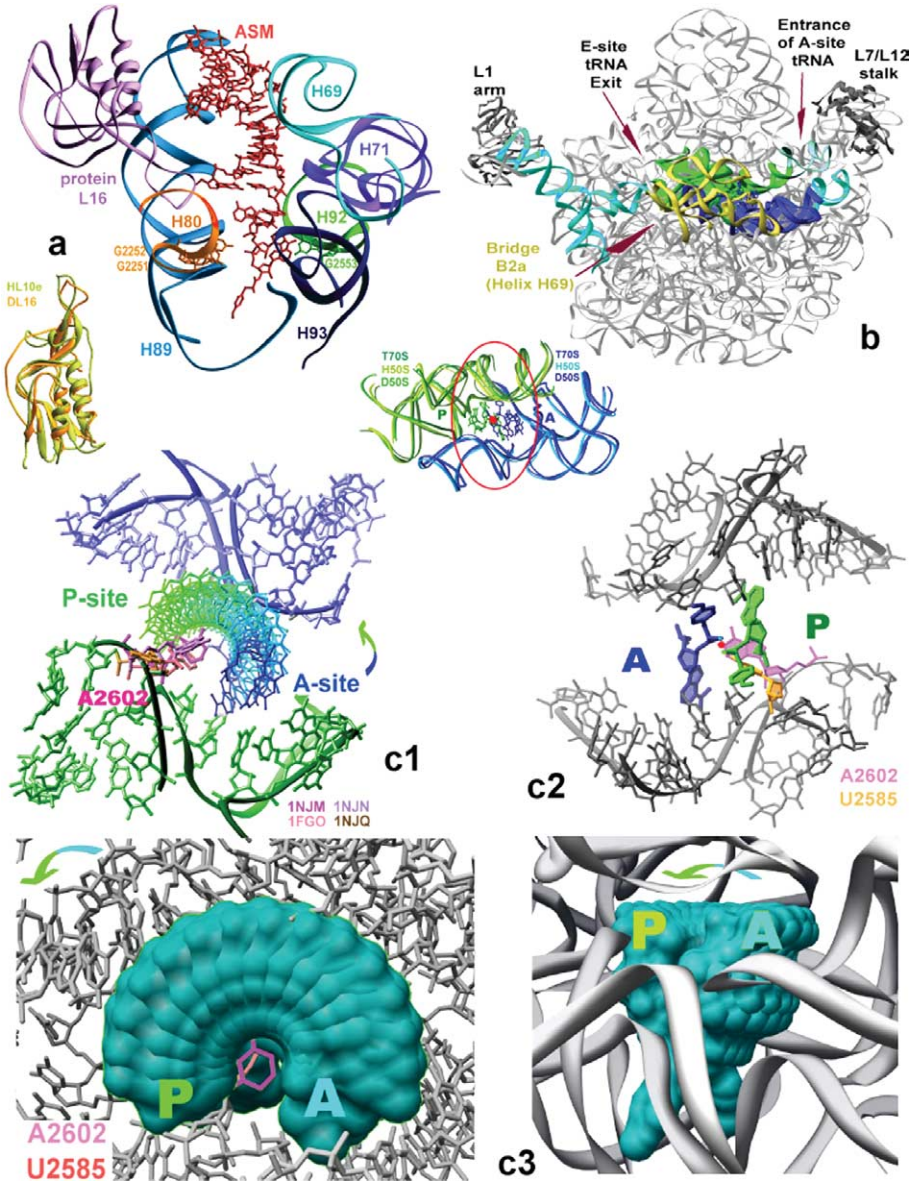

Fig. 1. (a) The PTC cavity in D50S complexed with ASM [1]. The nucleotides forming basepairs with A- and P-site tRNAs are numbered. Inset: Superposition of D50S protein L16, the only protein residing in the PTC cavity (a), and its mate in H50S, called L10e. (b) Bottom: A superposition of the RNA backbone of the symmetry-related region in all known structures [3,27,30]. The sub-region containing the A-loop is shown in blue and that containing the P-loop in green. The symmetry axis is red. The view shows also the ASM 3′ end at the A-site (blue) and the derived [1] P-site tRNA 3′ end (green), as atoms. The red ring designates the approximate PTC limits. Top: The symmetry-related region within D50S (filled by blue and green). Its extensions are colored cyan. Bring b2a (also called H69 tip); the bridge connecting the large subunit with the decoding region in the small subunit is yellow. Note that this bridge is also part of the PTC cavity upper rims (a). (c) Various presentations of the region encircle in red (b, bottom). In all, the A- and P-site components are shown in blue and green, respectively. A2602 and U2585 are marked whenever not covered by other features. The rotatory motion is illustrated by snapshots obtained by successive rotations of the aminoacylated-tRNA3′ end from A- (blue) to P-site (green) by 15° each, around the bond connecting the 3′ end with the rest of the tRNA molecule. The blue-green arrows indicate the direction of the rotatory motion. (c_1) The PTC boundaries scaffolding the path of the rotatory motion are colored according to the symmetry sub-regions, as in (b). In (c_{2-4}) ribosomal features are shown in gray. The rotatory motion anchors, A2602 and U2585, are highlighted in pink and magenta. Four different conformation of A2602 are shown in (c_1), with their PDB accession codes. In (c_1) the A- to P-site pass is represented by the gradual transfer from blue to green, whereas in (c_3) the volume taken by the rotatory motion is depicted in cyan. (c_2) The central part of (c_1), viewed from bottom, focusing on the geometry of the peptide-bond formation site. (c_3) Two orthogonal views illustrating the support and guidance given by the ribosome to the rotatory motion, highlighting the space allocated to this motion within the very crowded neighborhood (left), and the architectural design of the tRNA backbone, on the right. The rotatory motion is represented by the snapshots shown in (c_2), space filled in cyan.

guanines (G2251 and G2252) in orientations suitable for basepairing with the flipped CCA-end (Fig. 1a), instead of the single basepair donor (G2553) at the A-site [13]. Indeed, C75 of the derived P-site tRNA 3′ end [1] can readily basepair with G2251, and the base of C74 is facing that of G2252, so that only a minor rearrangement is required for the creation of a basepair between them.

A-site-tRNA C75 basepairing was observed in all complexes studied so far [1,14], manifesting its crucial role in substrate positioning. Nevertheless, this basepairing may not be suffi-

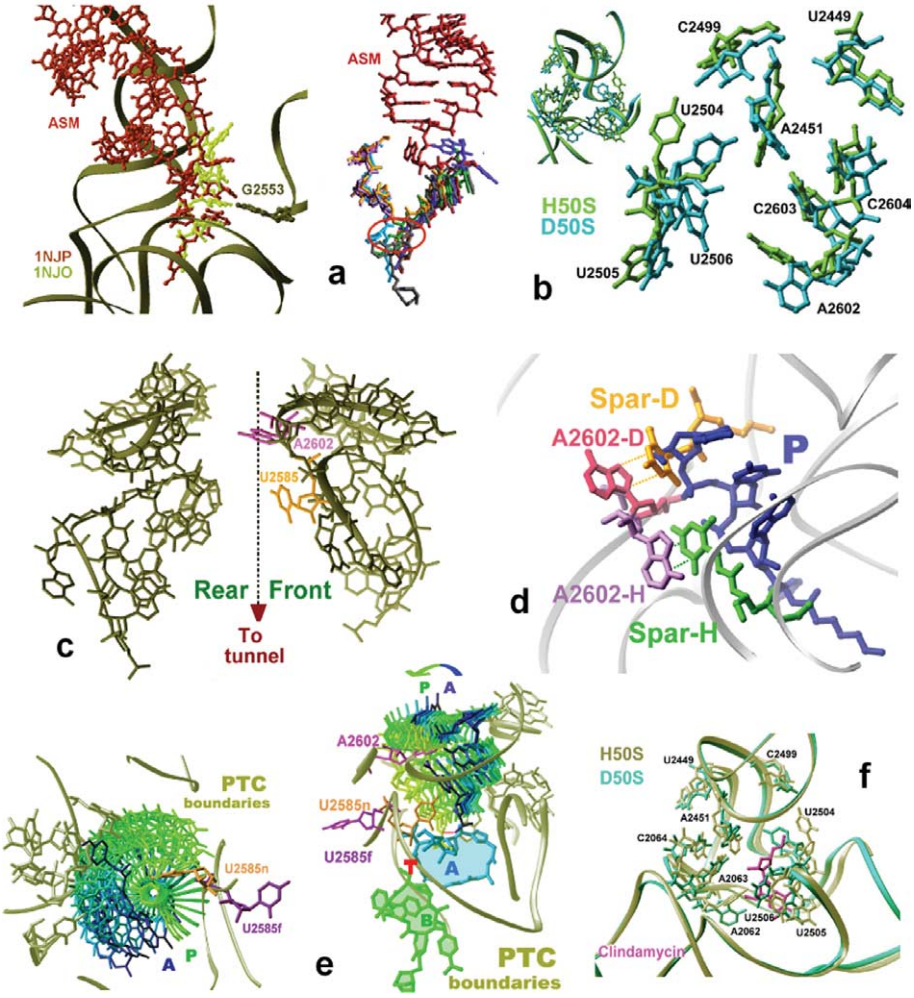

Fig. 2. (a) Left: superposition of a long (ASM) and a short tRNA mimics in D50S-PTC [1], together with the rRNA features in their proximity, including the universal basepair donor. Note that although both compounds are involved in this basepair, their orientations display considerable differences. Right: same as in the left, but including substrate analogs bound to H50S [14]. Note the similarity in their overall locations and the differences in their orientations in the region of peptide bond formation (encircled). (b) Superposition of the PTC nucleotides in H50S [14] and D50S [3]. Inset: the overall view. (c) A view perpendicular to of the PTC wall. (d) Sparsomycin binding sites in D50S (Spar-D) and H50S (Spar-H), illuminating the connection between the binding modes and the ribosome functional states. The ribosomal components are shown in gray. (e) Two orthogonal views of D50S PTC, together with the rotating moiety, as shown in Fig. 1c, focusing on the conformational alteration of U2585 (from U2585n to U2585f) induced by streptogramin$_A$ component of the synergetic antibiotic Synercid. Streptogramin$_B$ is shown on the right, indicating the mode of synergism enhancing the antibiotic action. The dotted line designates the approximate location of the new peptide bond and T represents the upper side of the tunnel. (f) Clindamycin-binding site on the superposition of H50S and D50S PTC.

cient for peptide-bond formation stereochemistry, since it can be created by tRNA 3′ end analogs, such as the fragment reaction reactants while placed at diverse orientations (Fig. 2a), most of which requiring conformational rearrangements [14]. In contrast, productive substrate orientation has been observed for a substrate analog mimicking the tRNA acceptor-stem, such as ASM, a 35 nucleotides substrate analog mimicking the A-site tRNA acceptor stem and its aminoacylated 3′ end (Fig. 1a). The detection of approximate symmetry in complexes with partially disordered or inaccurate intermediates [14] or with tRNA analogs too short to reach the PTC upper side demonstrates the relative ease of accommodating compounds resembling tRNA-3′ end in the PTC [15,16], and rationalizes the need for exploring five different H50S–puromycin complexes for discovering the need for additional rearrangements of such analogs.

We conclude, therefore, that global tRNA placement is dictated by its size and shape and the tRNA-CCA-end basepairing determines its approximate location within the symmetrical ribosomal frame. The fine-tuning of the correct aminoacylated-3′ end positioning, mandatory for efficient peptide-bond formation, is governed by remote interactions of the tRNA acceptor-stem with the PTC upper rim [15,16]. Consistent with recent findings that mutations in PTC nucleotides proximal to the catalytic site do not influence the rate of peptide-bond formation by tRNA molecules, but cause substantial increase in reaction rate when short tRNA analogs serve as substrates [11]. This hierarchy suggests that controlling accurate substrate positioning by remote interactions is designed for allowing PTC flexibility required for its various functions.

3. PTC flexibility, conformation rearrangements and chirality

The placement hierarchy hints that the PTC may be involved in substrate reorganizations when the initial orientation cannot

undergo the rotatory motion. Such rearrangements are bound to consume time, causing low rate of peptide-bond formation by short puromycin derivatives [11,14]. PTC involvement in substrate rearrangement requires considerable flexibility, consistent with PTC conformational variability observed in the different crystal structures (Fig. 2b) [3,17], which could be connected to active–inactive transitions revealed three decades ago [18] and reconfirmed recently [19].

Two universally conserved nucleotides, U2585 and A2602, shown to be essential for chain elongation [20] and E-site tRNA release [21], respectively, bulges out towards the symmetry axis and display remarkable flexibility (Figs. 1c and 2c) [1,2,5–7]. A2602 is a likely candidate for generating PTC conformation-alterations as it was shown to posses a different conformation in each complex studied so far (Fig. 1c) [1,5,15–17]. It is the only ribosomal entity interacting with sparsomycin, and its binding modes to D50S [1] and H50S [22] provide an excellent example for antibiotics binding mode that depends on the ribosomal functional-state. By entering non-occupied PTC, sparsomycin stacks to A2602 and causes striking conformational alterations in the entire PTC, influencing, in turn, the positioning of A-site tRNA [1,5,7]. Conversely, simultaneous binding of sparsomycin and a P-site analog seems to reduce the PTC mobility and enhance P-site-tRNA attachment (Fig. 2d).

At the PTC lower end, the flexible U2585 anchors the rotating-moiety at its aminoacid end. By exploiting its exceptional flexibility for creating unproductive interactions, A2585 may be involved in D-isomers exclusion [7,23]. An additional example showing U2585 importance is the need to construct the synergetic antibiotics Synercid with streptogramin$_A$/streptogramin$_B$ ratio of 70/30. Thus, upon binding to D50S, the streptogramin$_A$-compound known to hamper PTC activity, nucleotide U2585, undergoes a ~180° flip PTC [7,23] (Fig. 2e). This striking swing should prohibit U2585 involvement in the rotatory motion, and consequently trigger ribosomal counter attempts, rationalizing its poor inhibitory activity. Only by the addition of the streptogramin$_B$ component, which blocks the tunnel and interacts intensively with the streptogramin$_A$ component, thus hampering the escape of streptogramin$_A$, this drug acquires it's full potent activity. In contrast, streptogramin$_A$ causes hardly any U2585 motions in the PTC of *Haloarcula marismortui* [24], an archaeon sharing properties with eukaryotes. Since streptogramin$_B$ does not bind to H50S tunnel due to phylogenetic reasons, i.e. the key nucleotides for binding streptogramin$_B$ compounds, 2058, is a guanine instead of the eubacterial adenine, synergisms cannot be obtained. Different streptogramins$_A$ binding modes in ribosomes from H50S and D50S, representing two kingdoms of life is consistent with the inability of the PTC of H50S to bind typical eubacterial A- and P-sites antibiotics, such as chloramphenicol, clindamycin (Fig. 2f) [25] and tiamulin [26]. Thus, reconfirming that the PTC possesses considerable conformational variability despite its high sequence conservation [3,27].

4. The voyage through the exit tunnel

The entrance to the tunnel providing the path taken by nascent proteins until they emerge out of the ribosome is adjacent to the PTC (Fig. 3a–g). Recent biochemical studies indicate the tunnel ability to function as a discriminating gate for exporting proteins, to be involved in co-translational folding events, to respond to cellular signals and to regulate ribosomal interactions with the ER membrane [28,29], contrary to previous assumption that the tunnel is a passive path [30].

The spiral nature of the symmetry-related region ensures nascent proteins entry to the tunnel at a β-strand conformation, complying with the tunnel narrow entrance. In specific cases, likely be connected with nascent-chain–tunnel interactions, motions of rigid residues, such as prolines, may be restricted [31]. Shortly after entering the tunnel, the nascent peptides pass near a crevice of a size suitable for imitating nucleation of a few aminoacids at early stages of tunnel passage (Fig. 3a and b). The boundaries of the crevice are well defined, yet it may be associated with temporary tunnel-diameter expansion, as observed recently [32].

The tunnel walls are made mostly from rRNA, penetrated by mobile extended loops of several r-proteins (Fig. 3a, g) that appear to play key functional roles in the progression and cotranslational folding of nascent chains. Thus, a swing of L22 β-hairpin tip across the tunnel around an accurately placed hinge (Fig. 3c) [7,31] appears to provide the mechanism for elongation arrest, when triggered by specific cellular conditions [33]. Protein L22 has a long β-hairpin [34,35], which extends in the ribosome to the proximity of the tunnel opening (Fig. 3a) [6,31], hence can provide a communication route for signaling between the ribosome and the cell. Together with L4, L22 creates a dynamic tunnel-constriction, located at the deeper end of the hydrophobic crevice. Neither L22 nor L4, known to be involved in macrolide-antibiotics resistance [36,37], interacts directly with typical macrolide-antibiotics [23]. However, their involvement in resistance to macrolides, ketolides and azalides [38,39] can be explained by the interplay between them, since the swung conformation of L22 β-hairpin tip facilitates its interactions with L4 (Fig. 3d) [40,41]. Moreover, superposition of the structures of the L22 deletion-mutant acquiring erythromycin resistance on D50S led to the identification of a novel resistance mechanism, based on modifications of a location that is not adjacent to the antibiotics binding site, namely the increase of the tunnel diameter without corrupting the erythromycin-binding site, thus providing sufficient space for erythromycin and the growing chain.

5. 2058 is not alone

Macrolide-antibiotics, which rank highest in clinical usage, bind to a pocket located between the hydrophobic crevice and the tunnel constriction and block nascent proteins progression in eubacteria (Fig. 3e) [25,31,42,43]. Compared to the PTC, the tunnel is less conserved. Hence, phylogenetic diversity plays a considerable role in antibiotics selectivity and efficiency. The identity of nucleotide 2058 (A in all eubacteria, G in eukaryotes and archaea, including *H. marismortui*) is the key parameter for macrolide selectivity, since no typical macrolide binds to a tunnel with G2058. Consistently, A → G mutation or posttranslational methylation of A2058 acquire resistance to typical macrolides [44]. Chemically modified macrolides, such as ketolides and azalides designed to combat mac-

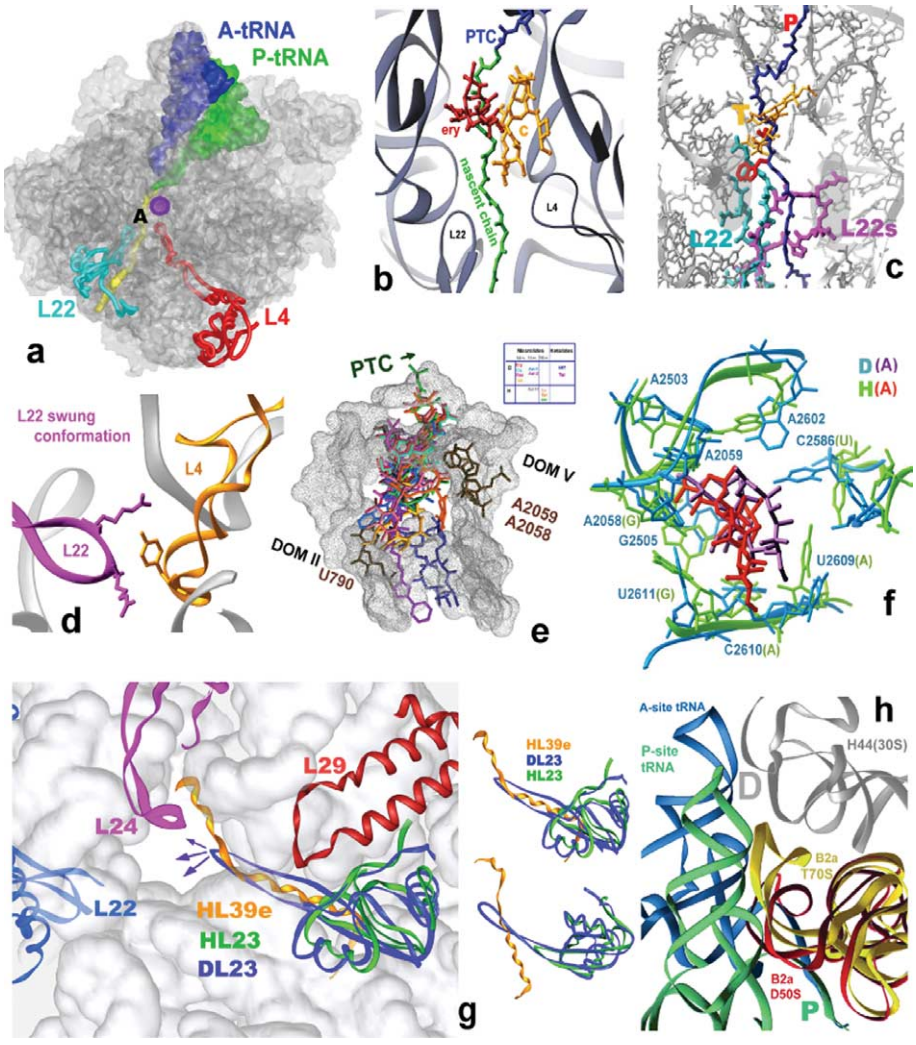

Fig. 3. (a) A section through the large ribosomal subunit (in gray), with docked A- and P-site tRNAs [27] and modeled nascent chain [29]. The approximate location of the crevice is indicated by a purple circle, and of the macrolide antibiotics binding site by the letter A. (b) The detailed structure of a section of the tunnel, between the PTC and the tunnel constriction, with the tips of L4 and L22 extended loops, as in (a). C: crevice, ery: erythromycin. (c) A view into the tunnel (gray), showing the antibiotic troleandomycin (T, yellow) that induces swinging (magenta) of protein L22 β-hairpin tip (native orientation in cyan). A modeled polypeptide chain (blue) represents a nascent protein with the sequence motif known to cause SecM (secretion monitor) elongation arrest, located about 150 residues from the N-terminus in XXXXXWXXXXXXXXXP, where X is any aminoacid, W is tryptophane and P (proline) is the last aminoacid to be incorporated into the nascent chain. The gray shaded areas show the approximate locations of the mutations that alleviate the elongation arrest [31]. The arrest essential proline and tryptophane are highlighted in red. (d) Possible interactions between L22 swung conformation and L4. The ribosomal RNA is shown in gray. (e) The binding modes of several antibiotics within a cross section of the ribosomal tunnel (doted gray cloud) at the level of the macrolides-binding pocket. The key nucleotides for macrolide–ketolide binding in domains V (DOM V) and II (DOM II) are marked. For orientation, the approximate PTC location is shown. D and H designate D50S and H50S, respectively. Ery: erythromycin; Cla: clarithromycin; Rox: roxithromycin; TAO: troleandomycin; Azi: azithromycin (Azi-1 and Azi-2: the primary and secondary sites of azithromycin in D50S), Azi-H: azithromycin site in H50S; ABT: ABT-773; Tel: telithromycin; Tyl: tylosin, Spi: spiramycin; Car: carbomycin. (f) Azithromycin main binding pocket in D50S (D(A) = pink on cyan) and H50S (H(A) = red on green), highlighting the differences in nucleotide type and orientations. (g) Left: the tunnel opening (light gray cloud) in D50S. The structures of L23 in H50S and D50S (HL23 and DL23, respectively) are superposed. Two different views of proteins H23 and HL39e (that exists only in H50S) are shown on the right and indicating that although HL39e appears to overlaps the extended loop of DL23, points deeper into the tunnel and occupies only a small part of the volume taken by L23 loop. The arrows show the direction of the allosteric motion induced by TF binding to L23 globular side, at the ribosome exterior. (h) The conformations of bridge B2a (H69) in the whole ribosome (yellow) [27] and in D50S (red) [3] together with A- and P-sites tRNA (as in [27]). The PTC (P) and the decoding site (D), on H44 of the small subunit (30S), are shown in gray.

rolide resistance, overcome it by interacting with other regions of the ribosomal tunnel (Fig. 3e).

The therapeutic effectiveness of macrolide derivatives that bind to resistant pathogenic strains is explained by differences in binding-modes to eubacteria versus eukaryotes or archaea. Importantly, within the macrolide-pocket of H50S, in addition to the principal difference in 2058 identity, the identities of seven nucleotides differ from their mates in typical eubacteria. Among them three are of the opposite type (namely purines instead of pyrimidines and vice versa). Furthermore, most of the conserved nucleotides have different conformations (Fig. 3f). Consequently, whereas macrolides block most of the D50S tunnel [23,25,31,40–43], those that bind to H50S occupy a smaller part of it (Fig. 3f) [40,41] demonstrating the influence

of conformational variability on drug efficiency. Thus, whereas 2058 identity together with macrolide modification determines whether binding occurs, the conformations of the proximal nucleotides govern binding-modes and drug effectiveness.

6. Nascent-protein emergence and elongation termination

While being elongated, nascent polypeptides portions reaching the tunnel opening interact with ribosome-associated chaperones assisting the folding process [45,46]. In eubacteria, the trigger-factor (TF) is the first to fulfill this task for cytosolic proteins. A funnel with dimensions that should allow partial nascent-protein folding [47] was identified at the tunnel opening by investigating results of three-dimensional-image-reconstruction obtained almost two decades ago [48]. Recent crystallographic studies, performed on complexes of eubacterial TF binding domain with H50S [49] and D50S (D. Baram and E. Pyetan, to be published), indicate that a sheltered folding space is formed by TF binding. This space is available for chaperone-assisted folding at the tunnel opening, and is confined by TF contacts with the ribosome exterior, namely proteins L23 and L29.

L23 is among the few r-proteins displaying dramatic differences among the three kingdoms of life. Only in eubacteria it posses a sizable extended loop that penetrates from the subunit exterior into the tunnel wall (Fig. 3g) [3]. The fully extended H50S protein, L39e, occupies part of the space consumed by the bacterial L23 extended loop (Fig. 3g), while running roughly perpendicular to it. Consistent with biochemical assignments [50], TF interacts with L23 globular domain of D50S and H50S in a similar manner, due to the high structural and sequence conservation of this region. However, although in H50S this binding induces no conformational changes in ribosomal components [49], the structure of D50S complexed with TF suggests significant allosteric conformational alterations at L23 extended loop. These alterations vary the tunnel shape in a fashion that may control the rate and directionality of nascent proteins entrance into their folding site. They may also provide a communication path between nascent chains, the TF, the ribosomal tunnel and additional cellular components. The failure of the chimeric complex built of the archaeal H50S with eubacterial TF to reveal conformational alterations induced by TF binding, supports it's specificity to eubacteria kingdom. It also indicates that different ribosomal-associated chaperones may bind in a similar way, but their function in assisting protein trafficking into the folding cradle, is species or kingdom dependent.

Elongation termination is accompanied by the dissociation of the assembled ribosome to its two subunits; a process triggered by the attachment of EF-G together the ribosomal-recycling factor (RRF). The structure of D50S complexed with *D. radiodurans* RRF shows that RRF binding causes a considerable loss of order of the intersubunit bridge connecting the PTC with the decoding center (R. Zarivach, to be published). This bridge, called H69 or B2a, is a highly flexible [3,17], thus readily disordered, as in H50S wild-type [51]. It is likely that the ribosome benefits from H69 flexibility beyond its participation in intersubunit bridging. Its proximity to the A- and P-sites suggests that it acts as a "crane" assisting translocation [17]. This multi-task feature is also a constituent of the PTC cavity upper rim (Fig. 3h) and as such it is instrumental for accurate substrate positioning [1,6]. Linking H69 functional disorder with ribosome dissociation is consistent with our previous proposal that inducing disorder in pivotal features [17] is a common ribosomal strategy for avoiding unproductive events. Hence, we conclude that the creation and the disruption of bridge B2a are key events in the initiation and termination of protein biosynthesis.

7. Conclusions

Ribosomes are ribozymes that position their substrates at stereochemistry appropriate for peptide-bond formation, polypeptide elongation, and substrate-mediated catalysis. The identification of the internal sizable symmetrical region containing the ribosomal catalytic site, which provides the frame for substrate placement, suggests that ribosomes evolved from gene-fusion of two structurally similar catalytic domains. The PTC architecture implies spiral rotation of the aminoacylated-tRNA3′ end within a precisely designed pattern in concert with the sideways translocation of the mRNA/tRNA complex. Guided and anchored by ribosomal components, this motion directs nascent chains entry into the exit tunnel at extended conformation, complying with the tunnels narrow entry.

This tunnel possesses dynamic properties enabling its participation in polypeptide elongation and arrest, sequence discrimination and signaling to various cellular components, including the ER membrane. At the tunnel opening eubacterial cytosolic proteins undergo TF aided cotranslational folding, controlled by protein L23 mobility. Conformational alterations of the intersubunit bridge connecting the catalytic site with the decoding center, induced by the RRF, seem to play a key role in protein biosyntheses termination steps.

Comparative analysis of antibiotics interactions with a eubacterial pathogen-model and an archaeon sharing properties with eukaryotes showed that despite the ribosomal conservation, phylogenetic and conformational variations within the antibiotics binding pockets allow drug selectivity, hence facilitating therapeutical usage. Although the identity of nucleotide 2058 is the primary determinant for typical macrolides binding, subtle conformational differences in the macrolide pocket govern the antibiotics clinical effectiveness.

Acknowledgments: We thank Thomas Cech, Aaron Klug, Anders Liljas and Ilana Agmon for fruitful discussion, Anat Bashan for elaborate computations, Idit Oren and Maggie Kessler for graphic representations. Thanks are also due to all members of the ribosome groups at Weizmann Institute, Israel and at MPG, Hamburg. X-ray diffraction data were collected at ID19/SBC/APS/ANL and ID14/ESRF-EMBL. The US National Inst. of Health (GM34360), the Human Frontier Science Program Organization (HFSP: RGP0076/2003), and the Kimmelman Center for Macromolecular Assemblies provided support. A.Y. holds the Martin and Helen Kimmel Professorial Chair.

References

[1] Bashan, A., et al. (2003) Mol. Cell 11, 91–102.
[2] Agmon, I., Bashan, A., Zarivach, R. and Yonath, A. (2005) J. Mol. Biol. (in press).
[3] Harms, J., et al. (2001) Cell 107, 679–688.
[4] Cooperman, B.S., Wooten, T., Romero, D.P. and Traut, R.R. (1995) Biochem. Cell Biol. 73, 1087–1094.
[5] Bashan, A., et al. (2003) Biopolymers 70, 19–41.

[6] Agmon, I., et al. (2003) Eur. J. Biochem. 270, 2543–2556.
[7] Agmon, I., et al. (2004) FEBS Lett. 567, 20–26.
[8] Dorner, S., Polacek, N., Schulmeister, U., Panuschka, C. and Barta, A. (2002) Biochem. Soc. Trans. 30, 1131–1136.
[9] Weinger, J.S., Parnell, K.M., Dorner, S., Green, R. and Strobel, S.A. (2004) Nat. Struct. Mol. Biol. 11, 1101–1106.
[10] Sievers, A., Beringer, M., Rodnina, M.V. and Wolfenden, R. (2004) Proc. Natl. Acad. Sci. USA 101, 7897–7901.
[11] Youngman, E.M., Brunelle, J.L., Kochaniak, A.B. and Green, R. (2004) Cell 117, 589–599.
[12] Gregory, S.T. and Dahlberg, A.E. (2004) Nat. Struct. Mol. Biol. 11, 586–587.
[13] Kim, D.F. and Green, R. (1999) Mol. Cell 4, 859–864.
[14] Moore, P.B. and Steitz, T.A. (2003) RNA 9, 155–159.
[15] Yonath, A. (2003) Chembiochem 4, 1008–1017.
[16] Yonath, A. (2003) Biol. Chem. 384, 1411–1419.
[17] Yonath, A. (2002) Annu. Rev. Biophys. Biomol. Struct. 31, 257–273.
[18] Zamir, A., Miskin, R., Vogel, Z. and Elson, D. (1974) Methods Enzymol. 30, 406–426.
[19] Bayfield, M.A., Dahlberg, A.E., Schulmeister, U., Dorner, S. and Barta, A. (2001) Proc. Natl. Acad. Sci. USA 98, 10096–10101.
[20] Wower, J., Kirillov, S.V., Wower, I.K., Guven, S., Hixson, S.S. and Zimmermann, R.A. (2000) J. Biol. Chem. 275, 37887–37894.
[21] Polacek, N., Gomez, M.J., Ito, K., Xiong, L., Nakamura, Y. and Mankin, A. (2003) Mol. Cell 11, 103–112.
[22] Hansen, J.L., Moore, P.B. and Steitz, T.A. (2003) J. Mol. Biol. 330, 1061–1075.
[23] Zarivach, R., et al. (2004) J. Phys. Org. Chem. 17, 901–912.
[24] Harms, J., Schluenzen, F., Fucini, P., Bartels, H. and Yonath, A. (2004) BMC Biol. 2, 1–10.
[25] Schluenzen, F., Zarivach, R., Harms, J., Bashan, A., Tocilj, A., Albrecht, R., Yonath, A. and Franceschi, F. (2001) Nature 413, 814–821.
[26] Schluenzen, F., Pyetan, E., Yonath, A. and Harms, J. (2004) Mol. Microbiol. 54, 1287–1294.
[27] Yusupov, M.M., Yusupova, G.Z., Baucom, A., Lieberman, K., Earnest, T.N., Cate, J.H. and Noller, H.F. (2001) Science 292, 883–896.
[28] Woolhead, C.A., McCormick, P.J. and Johnson, A.E. (2004) Cell 116, 725–736.
[29] Etchells, S.A. and Hartl, F.U. (2004) Nat. Struct. Mol. Biol. 11, 391–392.
[30] Nissen, P., Hansen, J., Ban, N., Moore, P.B. and Steitz, T.A. (2000) Science 289, 920–930.
[31] Berisio, R., Schluenzen, F., Harms, J., Bashan, A., Auerbach, T., Baram, D. and Yonath, A. (2003) Nat. Struct. Biol. 10, 366–370.
[32] Gilbert, R.J., Fucini, P., Connell, S., Fuller, S.D., Nierhaus, K.H., Robinson, C.V., Dobson, C.M. and Stuart, D.I. (2004) Mol. Cell. 14, 57–66.
[33] Nakatogawa, H. and Ito, K. (2002) Cell 108, 629–636.
[34] Unge, J., et al. (1998) Structure 6, 1577–1586.
[35] Davydova, N., Streltsov, V., Wilce, M., Liljas, A. and Garber, M. (2002) J. Mol. Biol. 322, 635–644.
[36] Wittmann, H.G., et al. (1973) Mol. Gen. Genet. 127, 175–189.
[37] Gabashvili, I.S., Gregory, S.T., Valle, M., Grassucci, R., Worbs, M., Wahl, M.C., Dahlberg, A.E. and Frank, J. (2001) Mol. Cell. 8, 181–188.
[38] Bozdogan, B., et al. (2003) Clin. Microbiol. Infect. 9, 741–745.
[39] Pereyre, S., et al. (2002) Antimicrob. Agents Chemother. 46, 3142–3150.
[40] Yonath, A. and Bashan, A. (2004) Annu. Rev. Microbiol. 58, 233–251.
[41] Auerbach, T., Bashan, A. and Yonath, A. (2004) Trends Biotechnol. 22, 570–576.
[42] Schluenzen, F., Harms, J.M., Franceschi, F., Hansen, H.A., Bartels, H., Zarivach, R. and Yonath, A. (2003) Structure 11, 329–338.
[43] Berisio, R., Harms, J., Schluenzen, F., Zarivach, R., Hansen, H.A., Fucini, P. and Yonath, A. (2003) J. Bacteriol. 185, 4276–4279.
[44] Weisblum, B. (1995) Antimicrob. Agents Chemother. 39, 577–585.
[45] Hartl, F.U. and Hayer-Hartl, M. (2002) Science 295, 1852–1858.
[46] Frydman, J. (2001) Annu. Rev. Biochem. 70, 603–647.
[47] Eisenstein, M., et al. (1994) (Pifat, G., Ed.), Supramolecular Structure and Function, Vol. 4, pp. 213–246, Balaban Press, Rehovot.
[48] Yonath, A., Leonard, K.R. and Wittmann, H.G. (1987) Science 236, 813–816.
[49] Ferbitz, L., Maier, T., Patzelt, H., Bukau, B., Deuerling, E. and Ban, N. (2004) Nature 431, 590–596.
[50] Kramer, G., et al. (2002) Nature 419, 171–174.
[51] Ban, N., Nissen, P., Hansen, J., Moore, P.B. and Steitz, T.A. (2000) Science 289, 905–920.